ESD-TR-68-199

Semiannual Technical Summary

Seismic Discrimination

30 June 1968

Prepared for the Advanced Research Projects Agency
under Electronic Systems Division Contract AF 19(628)-5167 by

Lincoln Laboratory

MASSACHUSETTS INSTITUTE OF TECHNOLOGY

Lexington, Massachusetts

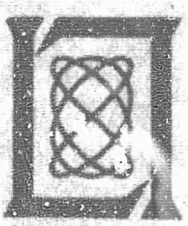

MASSACHUSETTS INSTITUTE OF TECHNOLOGY

LINCOLN LABORATORY

SEISMIC DISCRIMINATION

SEMIANNUAL TECHNICAL SUMMARY REPORT
TO THE
ADVANCED RESEARCH PROJECTS AGENCY

1 JANUARY – 30 JUNE 1968

ISSUED 22 JULY 1968

LEXINGTON MASSACHUSETTS

BLANK PAGE

ABSTRACT

Seismic source identification work during this reporting period has involved the development of several new analysis techniques for almost completely automatic production measurement on seismograms, and for less routine, more detailed studies. Studies of array signal detectability and signal and noise spatial character continue using data from both Montana (LASA) and Norway (NORSAR).

Accepted for the Air Force
Franklin C. Hudson
Chief, Lincoln Laboratory Office

CONTENTS

SUMMARY

This is the ninth Semiannual Technical Summary of Lincoln Laboratory's work for the Advanced Research Projects Agency on the seismic discrimination problem (Vela Uniform).

Identification studies using short-period and long-period small and large arrays are continuing. Means have been developed for applying the available simple waveform discriminant parameters to large numbers of events with a high degree of automaticity (Sec. I-A); to aid the search for new discriminants, a set of signal processing tools which provide a detailed dissection of individual events has been developed (Sec. I-B).

Work on detection and location at single stations has proceeded in several directions. LASA detection and two methods of LASA location were studied using data recorded during the Kuriles ocean bottom seismic experiment of late 1966 (Sec. II-A). A new processing method for high-resolution space-frequency analysis of signals or noise (Sec. II-B) has been developed; using this and other tools, a study of Montana long-period noise was completed (Sec. II-C). Recent studies of signal and noise properties of the Norway large array (NORSAR) site are reported in Sec. II-D. Section II-E summarizes the last three years' work on measuring and using LASA delay station corrections. A survey of work elsewhere on signal-to-noise improvement by seismometer emplacement in deep boreholes has been made (Sec. II-F).

A description of the latest work on the Seismic Data Analysis Console concludes this report.

P. E. Green

GLOSSARY

ARPA	Advanced Research Projects Agency
LASA	Large Aperture Seismic Array
LP	Long-Period
NORSAR	Norwegian Seismic Array
OBS	Ocean Bottom Seismometer
PDE	Preliminary Determination of Epicenter
SNR	Signal-to-Noise Ratio
SP	Short-Period
SPLP	Short-Period Long-Period
USCGS	United States Coast and Geodetic Survey
VESPA	Velocity Spectral Analysis

SEISMIC DISCRIMINATION

I. IDENTIFICATION

A. ARRAY IDENTIFICATION STUDIES USING LARGE EVENT POPULATIONS

Reports published earlier have described the application of long-period[1] and short-period[2] discriminants to LASA recordings of numbers of blast and earthquake events. The data base for those studies was obtained using two different computers, several different programs and multiple computer runs for each event. In order to continue such large population experiments and thus gain increased understanding of the existing discriminants, it was decided that the procedure should be significantly modified and simplified. Therefore, a single program (Short-Period Long-Period, or SPLP) has been written which will accomplish all routine long- and short-period analyses of array station (e.g., LASA) data in a single pass. The SPLP program also stacks data on a composite tape for future reference.

Figure 1 is a flow chart indicating all of the major operations done by the program.* Except for the entry of seismograms into core, no input or output has been shown. With respect to output it is sufficient to say that all measured or computed event parameters as well as beam waveforms and spectral curves are output graphically using an SC 4020 hard copy display, and are also stored on a composite tape. Although many options are available, only a small number of input parameters is changed for the routine processing of events. In particular, the program requires rough estimates of P arrival time, azimuth, and horizontal phase velocity for the event. Arrival times within 20 seconds are quite sufficient, and the estimated azimuth (β) and horizontal (v) phase velocity supplied to the program can be quite crude. When the quality of β and v are thought to be particularly poor, a larger grid of SP beams can be requested. Included in the outputs stored on tape are the unsmoothed amplitude spectral components of the first 20 seconds of the P-phase which are available for use in deriving possible improved versions of the spectral ratio discriminant.

The routine processing by SPLP differs in several ways, in addition to the obvious fact that much is automatic, from the processing done for earlier discrimination studies. The three most significant differences are the following. First, bandpass filtering is done by Fourier transforming, shaping, and inverse transforming rather than recursive or time domain convolutional filtering. Second, SP spectra are obtained by Fourier transforming and spectral ratio is obtained from the transformed data. Lastly, chirp filtering is done by applying a quadratic phase shift to Fourier transformed data and then inverse transforming rather than by time domain convolution.

A population of events detected and recorded at LASA has been compiled for analysis using

* SPLP will accept either Lo-Rate or Hi-Rate tape from LASA as input. If Lo-Rate tape is supplied, then both long-period and short-period analysis is done. Otherwise, only the short-period analysis is completed. The program requires about 20 minutes of IBM 360/67 time to completely process an event. This is reduced to 15 minutes if only short-period data are available. The program has been made sufficiently general so that it can be applied to short-period data recorded at other array sites with a minimum of effort.

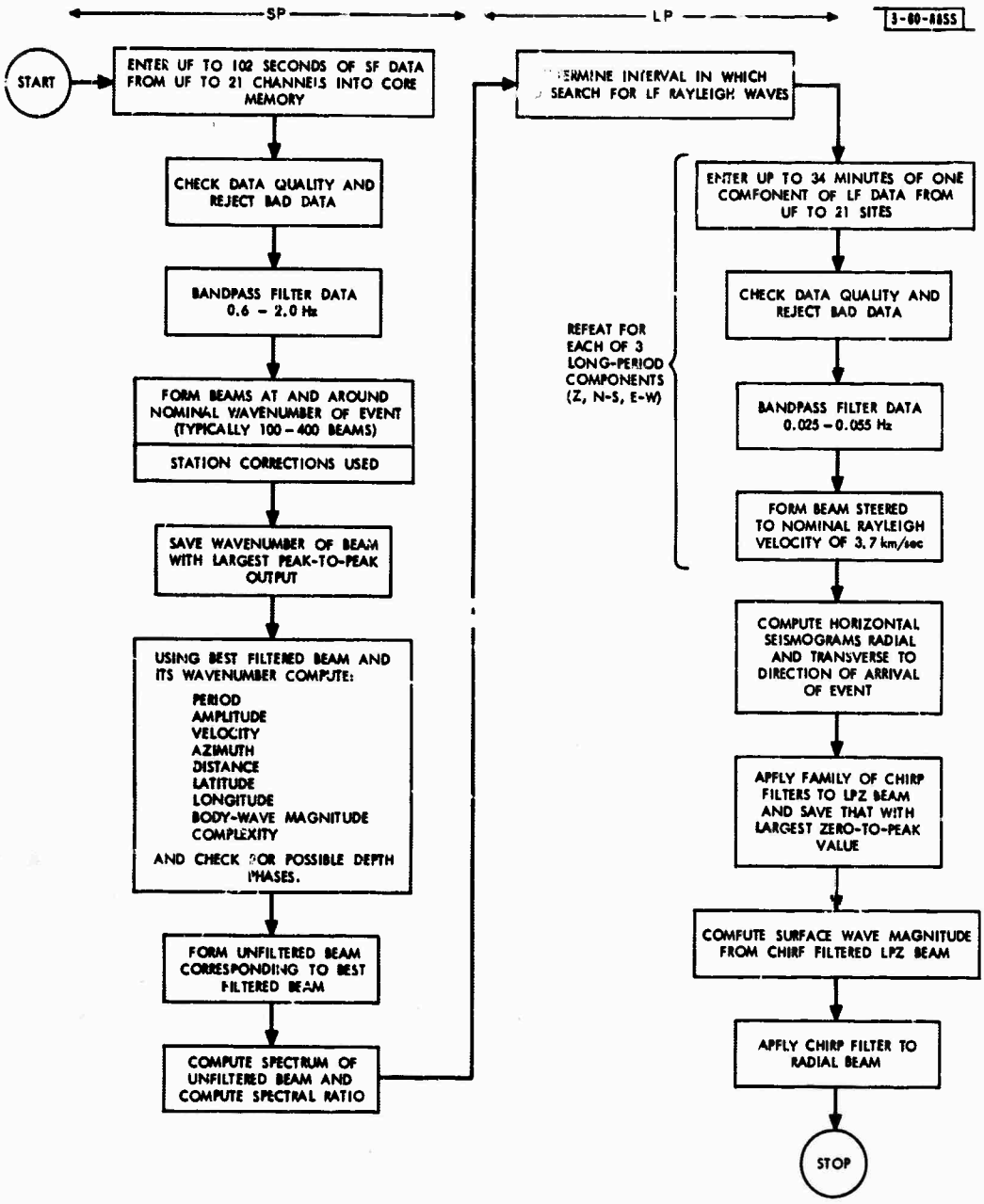

Fig. 1. Sequence of automatic seismogram reading operations in SPLP program.

SPLP. It includes some 30 teleseismic explosions, 35 large shallow Sino-Soviet events before 1968, and LASA-detected Sino-Soviet events between 1 January 1968 and 8 May 1968. So far SPLP has been successfully applied to more than 120 of the 175 events of this population that we intend to process.

R. T. Lacoss

B. SPECIAL METHODS FOR DETAILED ANALYSIS OF INDIVIDUAL EVENTS

The procedures described in Sec. I-A are being used to measure a few simple parameters on a large number of events for statistical evaluation. The "console" development, described earlier[3] and in Sec. IV-A, is motivated by a similar philosophy, namely the carrying out of a number of pre-programmed measurements on recorded data. In this Section we describe a series of programs based upon the contrasting approach of performing several very detailed analyses on the LASA waveforms of a small number of events in the hope of discovering details of the wave motion, as seen by the array, which may be made the basis of new discriminants. The emphasis is on providing useful hard copy displays, in addition to conventional seismograms, to be studied by a human observer. Three such displays, which are now in operation, will be described. They are all new and improved versions of techniques which have been described in previous reports.

The first is a velocity spectral analysis, called VESPA, which accepts 21 subarray waveforms and outputs signal power as a function of wave velocity and time. In this program, which replaces the "beam power display" described earlier,[4] 61 beams are formed from the bandpass filtered (0.6 to 2.0 Hz) subarray outputs, which may be weighted for control of array response. The beams are aimed at the bearing of the event being studied, at pre-assigned horizontal phase velocities corresponding to uniform increments in slowness of 0.2 second per degree, from 0 to 12 seconds per degree. Moveouts are computed from the 1968 Herrin-Taggart travel times and the best available station corrections are used. The beam outputs are formed once each LASA time sample (i.e., at 20 Hz) and its squares are summed over a 1-second time interval (integrate and dump) to produce output powers at a 1-Hz rate. These powers are summed between pre-assigned limits (say 20 seconds covering the main P-arrival) and displayed as a spectral density curve, i.e., power as a function of slowness. In addition, the 61 beam powers are treated as functions of time over one or more 1-minute frames and displayed as contour diagrams of power vs slowness and time. The contours are curves of constant numbers of db down from the peak value observed in the first minute, and the display shows the detailed variation with time of the distribution of signal power with respect to slowness.

In Fig. 2(a) we see such a 2-minute frame for an East Kazakhstan presumed underground test. The LASA D, E, and F rings were used, with weights applied to equalize the peak-to-peak amplitudes. Three of the constituent filtered seismograms are shown in Fig. 2(b). The total spectrum of power vs slowness for the 20-second interval marked on Fig. 2(a) is given in Fig. 2(c). The main lobe agrees very well, down to about 10 db, with a theoretical pattern for a wide-band source, monochromatic in velocity. Analogous displays are shown in Figs. 3(a), (b), and (c) for a presumed underground test at Novaya Zemlya, using the same collection of 12 LASA sensors. The event is much more complex, and signal energy with very nearly the P-velocity can be seen

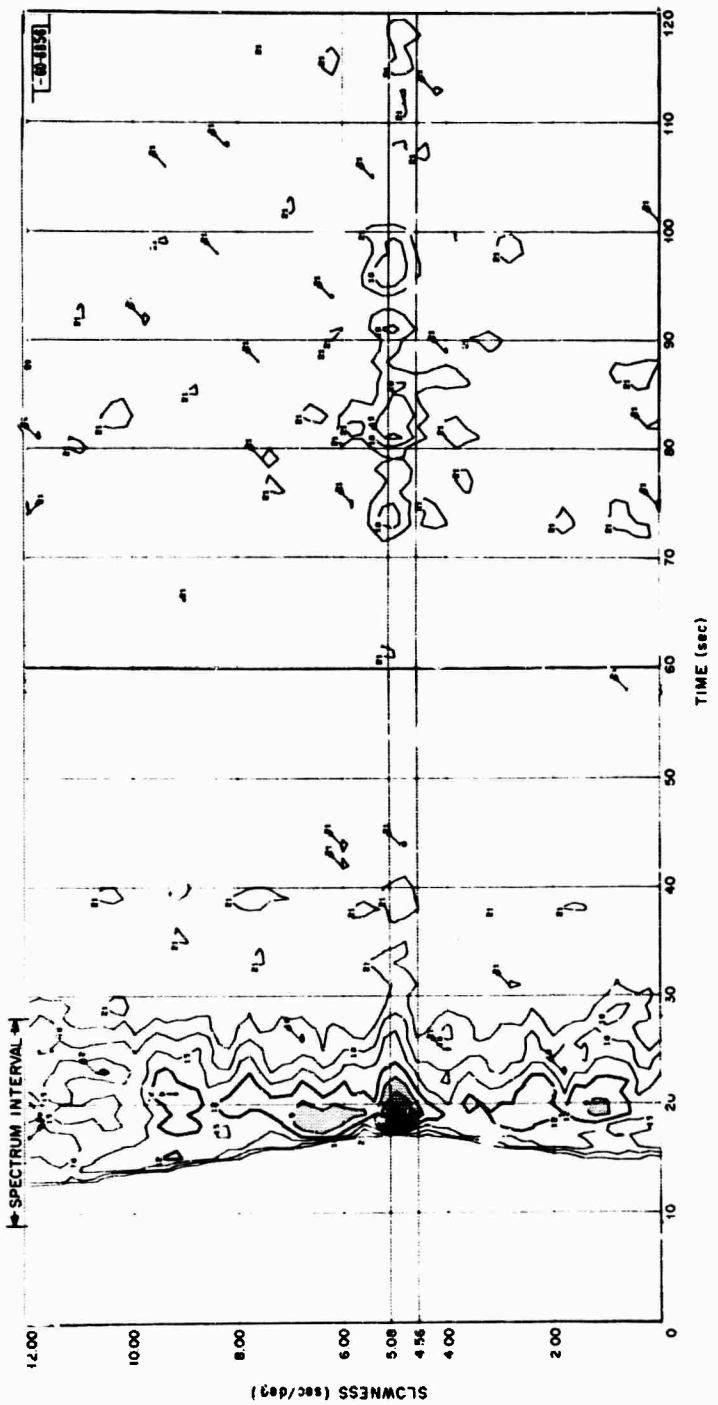

(a) VESPA – power versus arrival direction and time.

Fig. 2. Velocity spectral analysis (VESPA) and related quantities for an East Kazakhstan presumed underground test.

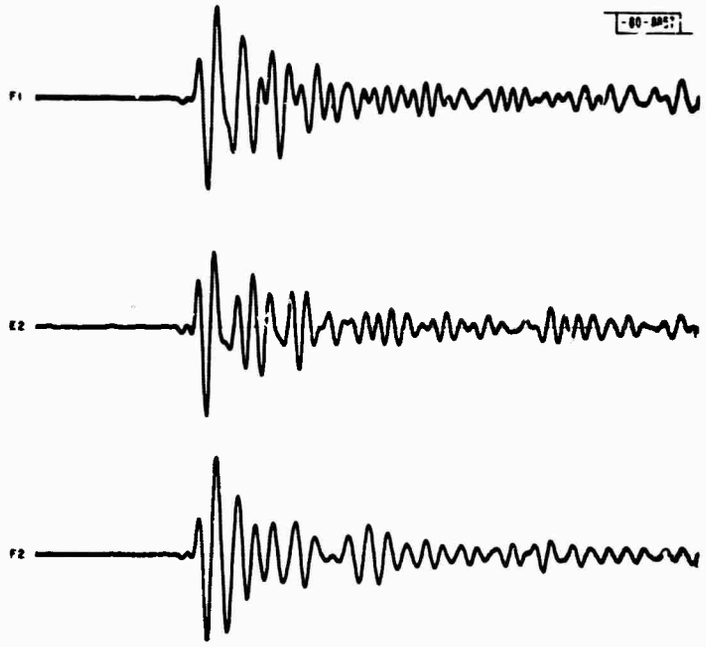

(b) Several filtered subarray outputs.

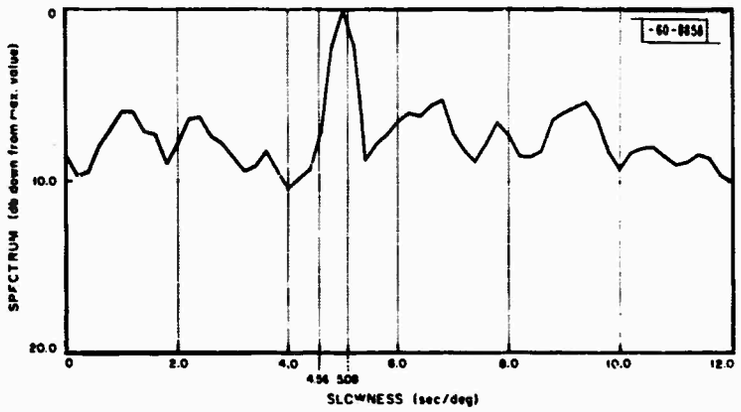

(c) VESPA integrated over the 20-second interval marked "SPECTRUM INTERVAL" in Fig. 2(a).

Fig. 2. Continued.

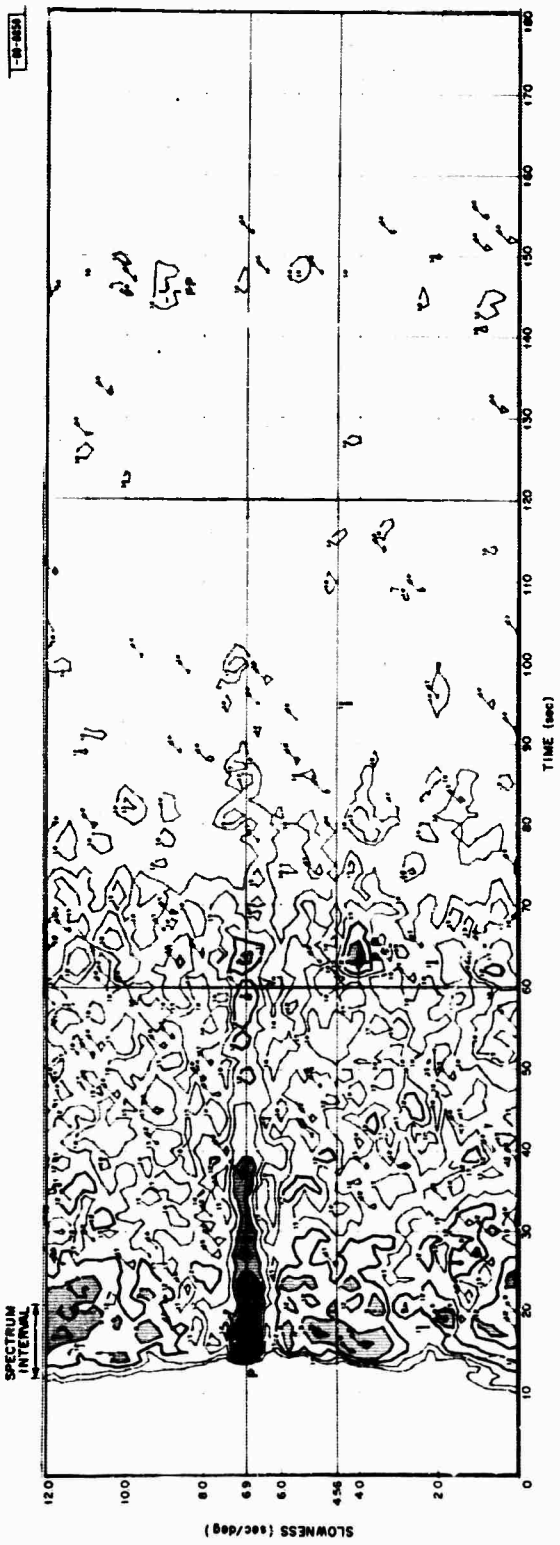

(a) VESPA – power versus arrival direction and time.

Fig. 3. Velocity spectral analysis (VESPA) and related quantities for a presumed explosion at Novoyo Zemlyo.

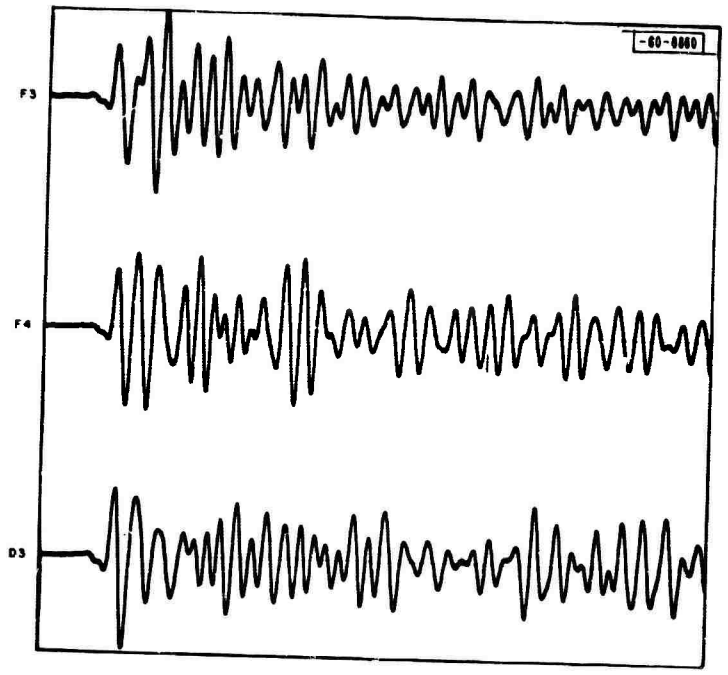

(b) Severol filtered suborroy outputs.

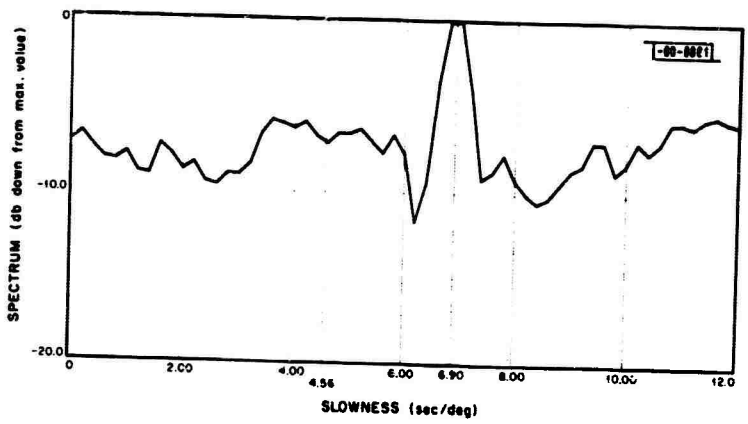

(c) VESPA integrated over the 20-second interval morked "SPECTRUM INTERVAL" in Fig. 3(a).

Fig. 3. Continued.

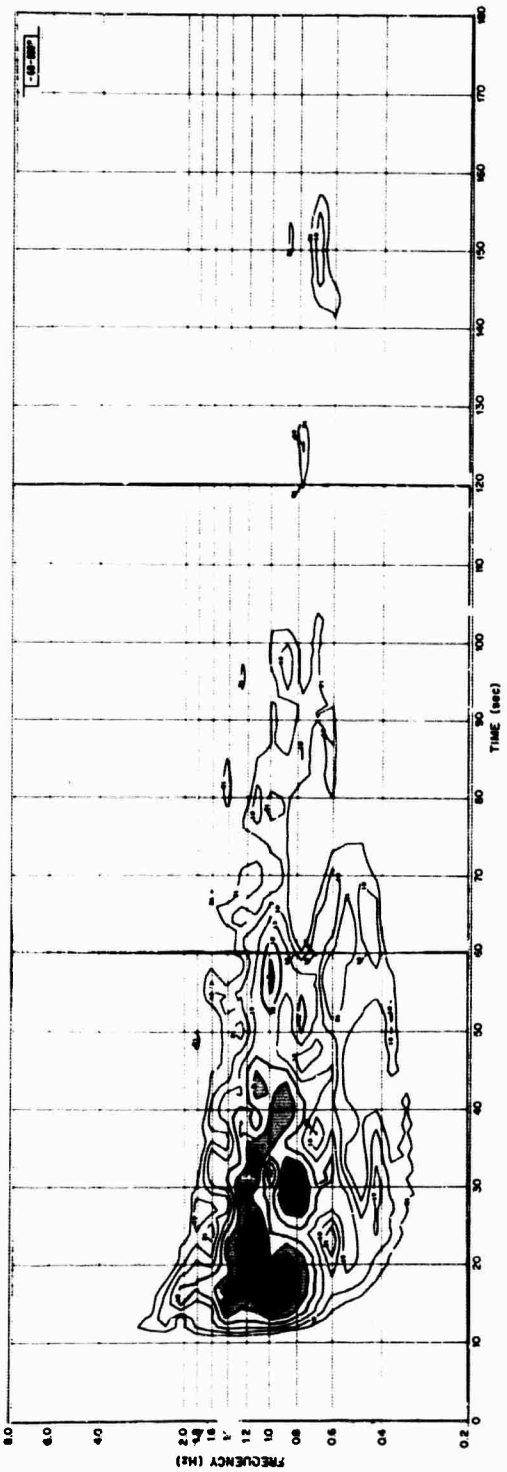

Fig. 4. Power vs frequency and time ("Sonogram") of the event analyzed in Fig. 3.

to arrive in substantial amounts for over 1 minute, while the first 20 seconds still show a reasonable velocity spectrum. The phases PcP and PP are also visible in the temporal display, which in this case shows 3 minutes of data.

The second display is a new version of the previously described "sonogram"[5] program. A single input waveform is passed through the digital equivalent of a bank of 31 narrow-band (three-pole Butterworth) filters, all having the same Q. The power output of each filter is summed for 1 second (20 samples) and these data are displayed as contour diagrams of power vs frequency and time for 1-minute frames, exactly as in the VESPA program. The program actually generates sonograms for up to five input channels simultaneously, and as usually applied, one channel is a preformed beam steered at the event. An example of the sonogram display, using the same Novaya Zemlya event of Fig. 3, is shown in Fig. 4. The characteristic delay in the arrival of lower frequency energy is due to the fact that all filters have the same Q (bandwidth is 10 percent of center frequency), hence the low-frequency filters have greater delay time. It has been observed that the frequency of peak energy varies considerably from subarray to subarray for a single event, and is only weakly correlated with the dominant period, as read from the original seismograms.

The third display is a particle motion analysis,[6] using the short-period triaxial sensors installed in subarray B2. The horizontal records are converted to radial and transverse components and particle motion tracings of vertical vs radial and radial vs transverse are generated for a sequence of 2-second frames. The expected angle of particle motion in the vertical-radial plane is displayed, along with raw seismograms and a time-smoothed version of the squared vertical trace. This last waveform is roughly similar to the AWRE correlogram[7] output.

None of these programs has as yet been run on significant numbers of events, but it is our intent to use them for detailed study of representative earthquakes and explosions in the hope of finding new P-waveform discriminants and of elucidating the structure of the P-coda.

E. J. Kelly
L. T. Fleck
P. E. Green

BLANK PAGE

II. SINGLE-STATION DETECTION AND LOCATION

A. COMPARISON OF LASA OBSERVATIONS WITH KURILES OCEAN BOTTOM NET OBSERVATORIES

The Kurile Islands offshore experiment conducted at the end of 1966 provided the opportunity of obtaining accurate locations of several small underwater explosions and many small local and near regional earthquakes from a seismically active area. This population of events has been used to better determine the Montana LASA beam detection threshold for teleseismic P waves and the epicenter location error by the use of both plane wave approximation to the arrival times at selected subarrays and beamsplitting. A detailed report on this work is in preparation.

The beam detection threshold for the Kuriles was obtained from 42 events thus far processed. If a seismicity curve with a unity slope is used, the 75 percent cumulative detection threshold is 3.8. If a curve is fit to the data, a slope of 0.75 is obtained with a 75 percent cumulative detection threshold of 3.65. Figure 5 summarizes the results.

The accuracy of epicenter location by either plane wave approximation (fitting a plane wave to individual subarray times) or beamsplitting is strongly affected by station time errors. Station corrections obtained from Teledyne were used to compensate for these time anomalies.[8] The plane wave epicenter locations produced epicenter errors shown in Fig. 6(a), while the epicenter location errors from the beamsplitting method are shown in Fig. 6(b). (See also Fig. 7 of the 31 December 1967 Seismic Discrimination Semiannual Technical Summary Report.) The epicenters obtained from the plane wave approximation method were computed to 0.1 degree; however, the epicenters obtained from the beamsplitting method are quantized to 0.5-degree increments of latitude and longitude such that the best beam must fall on one of these increments. The epicenter location error plotted for beamsplitting can be considered to be the upper bound of the location error because of the coarseness of the increments.

The data base used to get the above detection and location results contains 84 events that occurred in the Kurile Islands region between 23 October and 12 December 1966. The epicenters were obtained from four sources: (1) the Coast and Geodetic Survey PDE list, (2) Texas Instruments, Inc., analysis of ocean bottom seismometer (OBS) data,[9] (3) Lincoln Laboratory analysis of OBS data, and (4) the LASA station bulletin. The LASA station bulletin epicenters were considered the least accurate not only because of the limited baseline of the array, but also because the LASA epicenter location computer program had not been fully implemented with station corrections at that time.

A further discussion of category (3) is in order. In order to increase the number of small events contributed by the OBS data, epicenters were computed for sets of events not located by Texas Instruments. In order to locate these events, we assume a surface focus (Texas Instruments' location included a depth determination and, therefore, required detection at more of the OBS instruments) so that only two P arrivals and one S arrival were required to determine an epicenter.[10] If only two P arrivals and one S arrival are used, two epicenters are produced. Any additional readings serve to resolve the ambiguity and refine the epicenter. The accuracy of the resulting epicenters depends upon good P and S readings and upon a knowledge of the P_n speed and the S-P interval as a function of distance. We first attempted to get S-P intervals using the underwater explosions for which an accurate epicenter was known, but the resulting

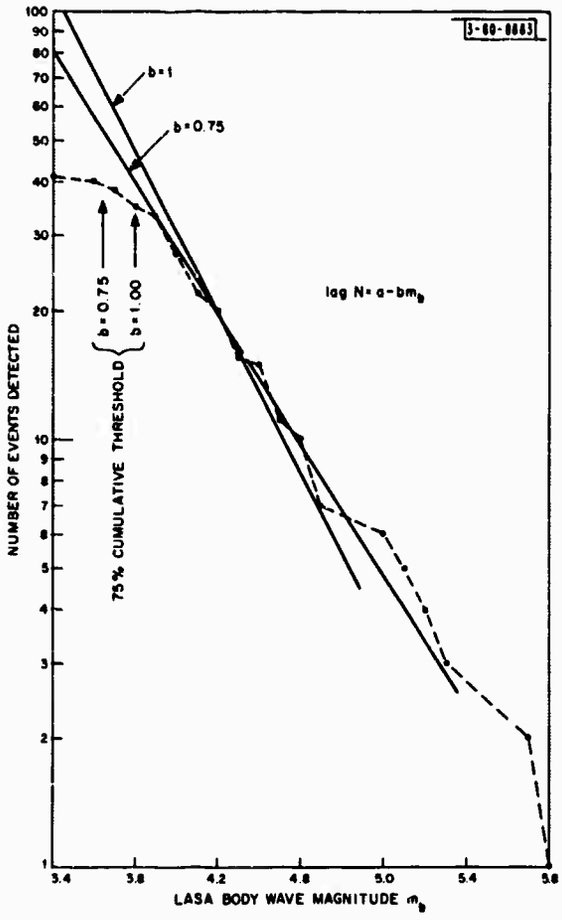

Fig. 5. Cumulative number of Kuriles events detected on Montana LASA beam outputs vs LASA magnitude.

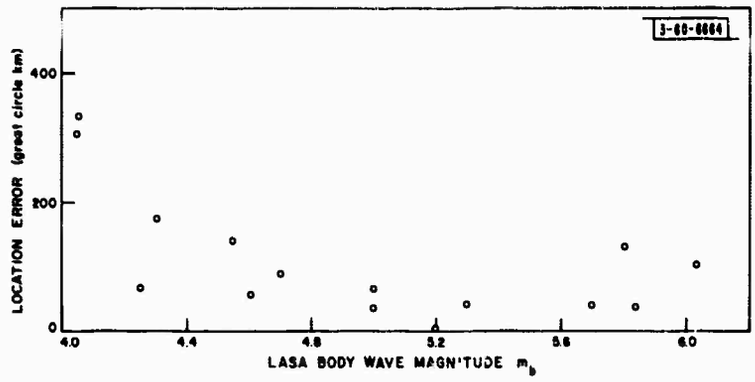

(a) LASA epicenters derived fram plane wave fit ta individual subarray times ("triangulatian").

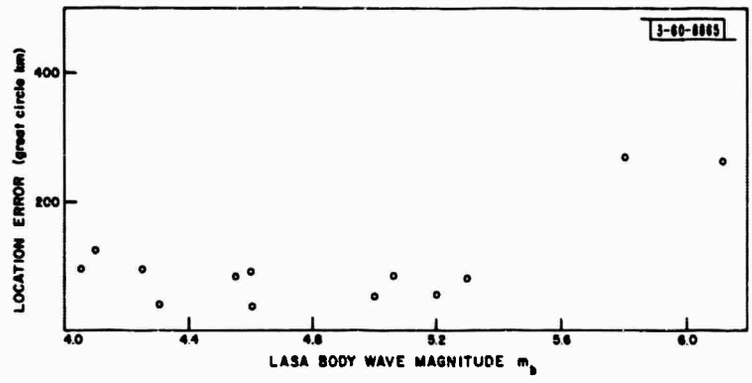

(b) LASA epicenters derived from beamsplitting (determining beam with largest autput).

Fig. 6. Disagreement between LASA epicenters and epicenters from either USCGS ar Kuriles acean battam seismometer net.

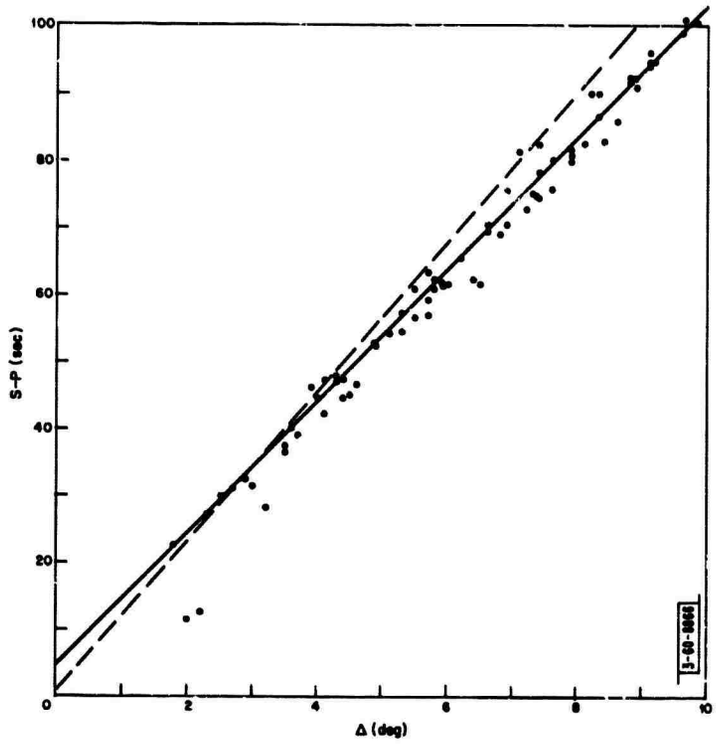

Fig. 7. Time intervals S-P derived from USCGS Kuriles epicenters and ocean bottom seismometer data.

S-P intervals showed a large scatter, probably because of the water part of the propagation path. The population of earthquakes located by the USCGS produced more consistent S-P intervals and enabled a good determination of the S-P separation with distance. Figure 7 shows the data and the resulting curve.

R. M. Sheppard

B. HIGH-RESOLUTION FREQUENCY-WAVENUMBER SPECTRUM ANALYSIS

The frequency-wavenumber spectrum of seismic noise provides the information about the distribution of noise power with frequency and for a fixed frequency reveals the velocity and direction of propagation of the noise. A high-resolution method for measuring the frequency-wavenumber spectrum of seismic noise has been developed. A detailed description of this program as well as the conventional method, have been given in a recent report.[11]

The conventional method of frequency-wavenumber spectrum analysis is based on the estimate

$$\hat{P}(f, \underline{k}) = \frac{1}{K^2} \sum_{j,\ell=1}^{K} \hat{f}_{j\ell}(f)\, e^{i\underline{k}\cdot(\underline{x}_j - \underline{x}_\ell)}$$

where f is the frequency, $\underline{k}$ is the vector wavenumber, K is the number of sensors, $\underline{x}_j$ is the vector position of the j^{th} sensor and $\{\hat{f}_{j\ell}(f)\}$ is the estimate of the spectral matrix of the noise. The high-resolution estimate is defined as

$$P'(f, \underline{k}) = \left[\sum_{j,\ell=1}^{K} \hat{q}_{j\ell}(f)\, e^{i\underline{k}\cdot(\underline{x}_j - \underline{x}_\ell)} \right]^{-1}$$

where $\{\hat{q}_{j\ell}(f)\}$ is the inverse of the spectral matrix $\{\hat{f}_{j\ell}(f)\}$. It can be shown that $P'(f, \underline{k})$ is the output of a maximum-likelihood filter, whose design is determined by the noise data and is different for each wavenumber $\underline{k}$, which passes undistorted any monochromatic plane wave travelling at a velocity corresponding to the wavenumber $\underline{k}$, and suppresses in an optimum manner the power of those noise waves travelling at velocities corresponding to wavenumbers other than $\underline{k}$. It should be noted that the amount of computation required to obtain P' is almost the same as that to get $\hat{P}$, since only an additional Hermitian matrix inversion is required.

Two examples which illustrate the results obtained with both the conventional and high-resolution frequency-wavenumber programs are given in Figs. 8(a) and (b). In both cases the entire long-period vertical array at LASA was employed. It has been shown that the noise in the 0.025- to 0.05-Hz band consists of a component propagating as fundamental-mode Rayleigh waves, and a nonpropagating or incoherent component.[11] Thus, the wavenumber structure of the noise, at a particular frequency, should consist of an arc, or arcs, whose extent corresponds to the range of the azimuths of the sources of the propagating component of the noise.

In Fig. 8(a) the noise is seen to consist primarily of a component propagating from the North. Hence, as expected, the conventional wavenumber results appear to be very similar to a LASA beamforming array response pattern. The high-resolution results delineate the wavenumber structure as a point source more clearly than does the conventional method. This figure

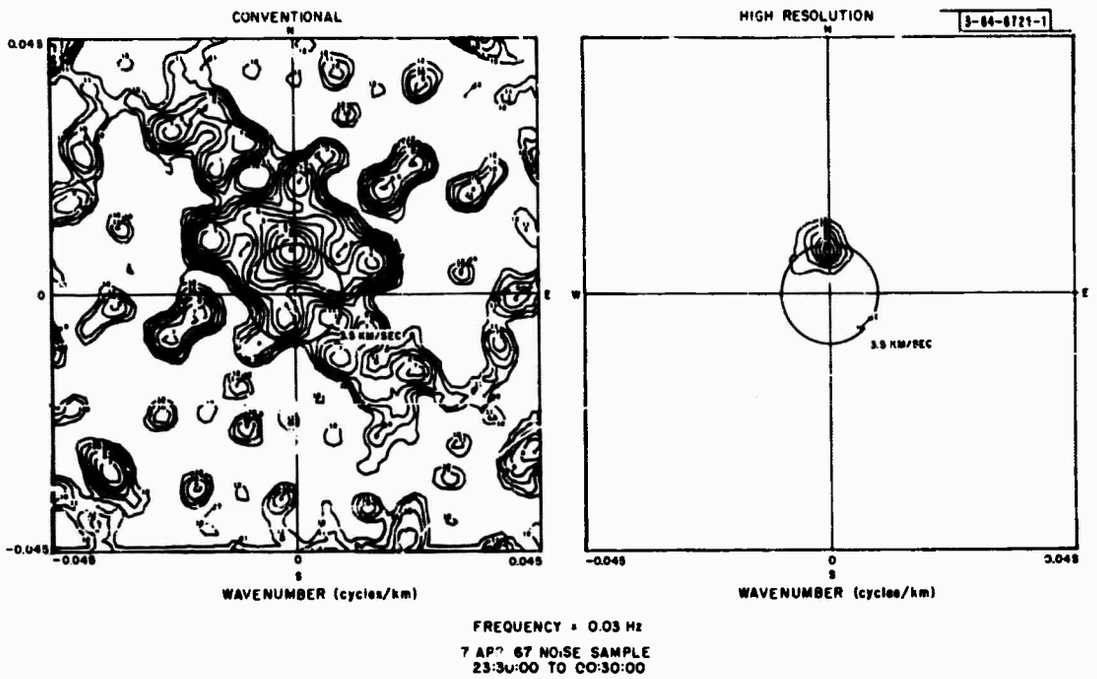

(a) Point urce.

Fig. 8. Comparison of conventional (left) and high resolution (right) LASA long-period array wavenumber plots for two interesting noise samples.

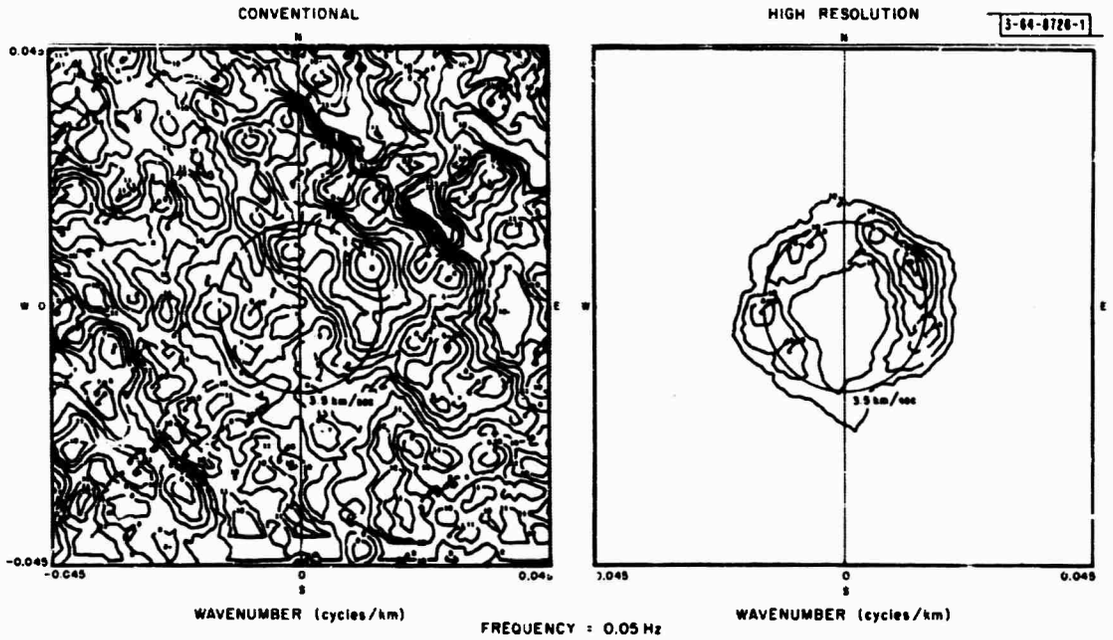

(b) Single velocity, all azimuths.

Fig. 8. Continued.

shows that there is an improvement in wavenumber resolution of the high-resolution method relative to the conventional method of about a factor of four. The results of Fig. 8(b) are also interesting, as they show a 360-degree azimuthal spread for the wavenumber structure with a variable energy density along this circle. In addition to the noise analysis, an effort is also in progress to apply the high-resolution method to the short-period P-wave data in an attempt to improve the location capability of large arrays.

J. Capon

C. NOISE MEASUREMENTS IN MONTANA

The long-period noise in the 20- to 40-second period range limits the identification level at which the surface-wave, body-wave discriminant can be applied at LASA. Therefore, an investigation was made to determine the sources and properties of this noise. Only the long-period vertical array at LASA was considered.

The conventional and high-resolution* frequency-wavenumber spectra of the noise were measured, as well as coherence. These data show that the noise consists of two components. One component propagates across the array as fundamental-mode Rayleigh waves and is thought to be caused by the action of surf on coastlines. The other component is nonpropagating and has been found to be incoherent over distances greater than 7.5 km.

It is important to establish the origin of the nonpropagating seismic noise since if means could be found to suppress it, thus exposing the propagating component more prominently, maximum-likelihood processing could be used effectively against the latter to improve LP detection thresholds. Previous results due to Haubrich and MacKenzie[12] indicate that the nonpropagating noise might be due to the elastic loading on the ground by the earth's atmosphere. Thus, an effort was made to determine the coherence between the seismic noise and the atmospheric fluctuations as recorded on microbarograph sensors at LASA.

Two examples in which coherence was measured at site AØ are given in Figs. 9(a) and (b), where Fig. 9(b) is more typical of the behavior of the coherency when any coherence is measured at all. In Fig. 9(a) the coherence at 0.03 Hz is quite high, about 0.6, and drops to about 0.5 and 0.4 at 0.04 and 0.05 Hz, respectively. The ratio of nonpropagating noise to the total noise, for this noise sample, was measured as 0.9 at 0.03, 0.04 and 0.05 Hz. The measured coherence is not as high as this at these frequencies, but is the largest that was ever measured in the 17 noise samples examined. The results of Fig. 9(b) are more typical in that whenever coherence is measured, it tends to be high at 0.02 Hz and then drops to the level for incoherent noise at 0.03 to 0.05 Hz. The ratio of nonpropagating to total noise for the noise sample used in Fig. 9(b) was measured as 0.60, 0.45 and 0.35 at 0.03, 0.04, and 0.05 Hz, respectively. The coherence never reaches a level compatible with the amount of nonpropagating noise. Thus, it may be concluded that there is relatively little coherence between the seismic noise and the microbarograph signals in the 20- to 40-second period range.

An attempt was made to correlate the amount of nonpropagating seismic noise power and the amount of microbarograph noise power in the 20- to 40-second period range. These quantities were measured at site AØ for 17 noise samples and the results are shown in Fig. 10. This figure

* See Sec. II-B.

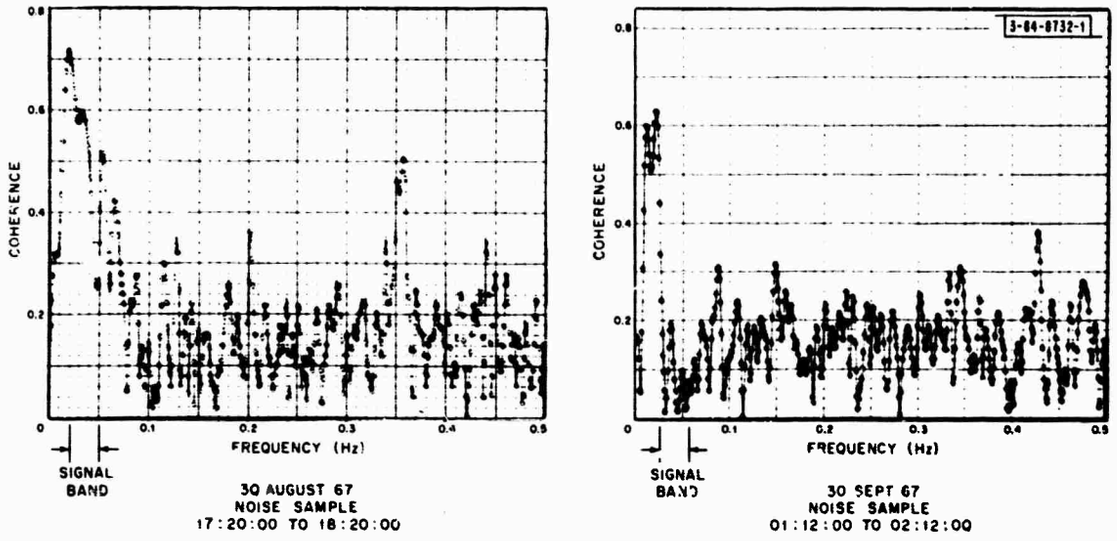

(a) (b)

Fig. 9. Coherence between outputs of LASA seismometer and nearby microbarograph.

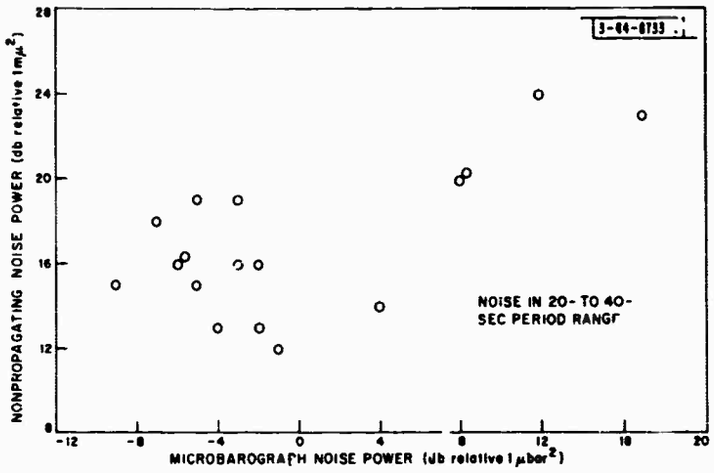

Fig. 10. Correlation between high nonpropagating LP noise levels and high microbarograph noise levels.

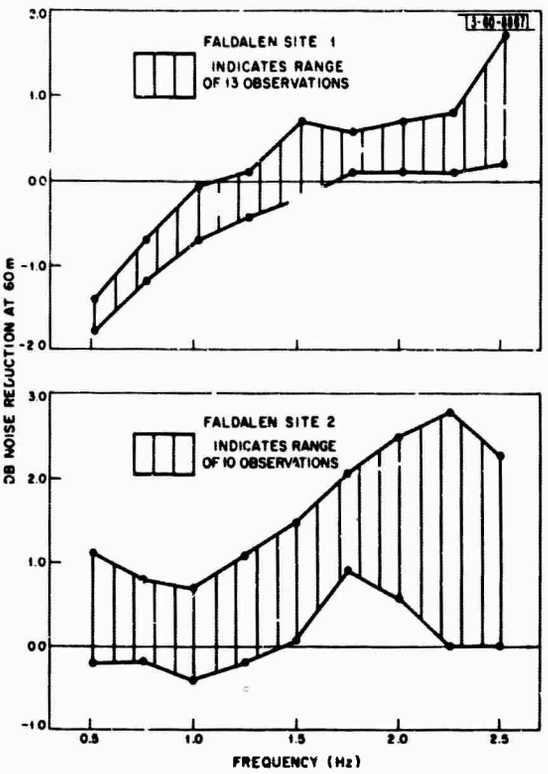

Fig. 11. Reduction in noise level at bottom of 60-meter Norway boreholes relative to 2-meter-depth "surface" elements, as a function of frequency.

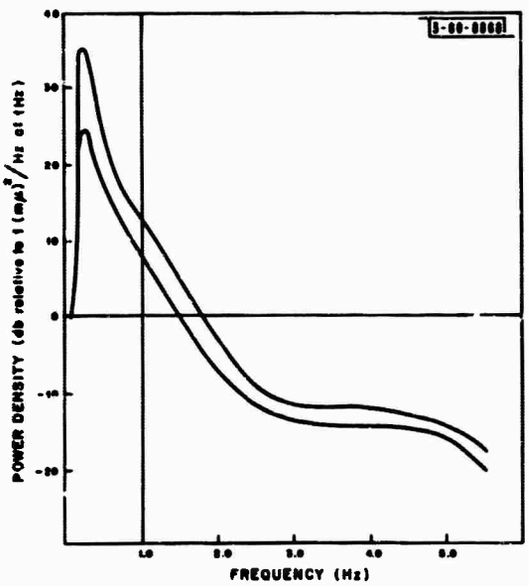

Fig. 12. Typical Norway noise spectrum. Maxima and minima of noise spectral level at Faldalen over 8-day period 2 November 1967 to 14 December 1967.

shows that there is a definite trend for the power level of the nonpropagating noise to increase when the power level on the microbarograph increases. Thus, this is evidence that the nonpropagating seismic noise is caused by the elastic loading on the ground by the earth's atmosphere. The nonpropagating seismic noise may be caused by the cumulative effects of many independent atmospheric pressure fluctuation cells within a radius of a few km of the seismometer and this may be the reason for the low coherence between this noise waveform and a single microbarograph record obtained at the same location.

A detailed description of these results has been included in a recent report[11] describing the technique discussed in the preceding section.

J. Capon

D. NORWAY SIGNAL AND NOISE PROPERTIES

Analysis of noise and signal data from the Norwegian Seismic Array (NORSAR) site has continued. The earlier short-period results[13] have been substantiated and extended. Some properties of the long-period noise and signal have also been obtained.

The effect of seismometer burial and local weather conditions upon noise levels has been thoroughly investigated using data from the Faldalen site. Our conclusion is that instruments which are 60 meters into bedrock will seldom, if ever, be more than 3 db quieter in the signal band than instruments only 2 meters into bedrock. Average and peak winds were obtained from data recorded by the Faldalen weather station from 28 December 1967 to 22 March 1968. Simultaneous spectra were obtained from instruments at 2 and 60 meters at the Faldalen site. The wind conditions during these measurements ranged from calm to periods with gusts to 45 mph and sustained winds to 24 mph. These latter conditions are among the most severe during the observation period. Figure 11 shows the range of noise attenuation that was recorded at the two 60-meter holes in the Faldalen site. It can be seen that almost 3 db of attenuation was obtained at least above 2.0 Hz at one of the 60-meter holes. However, below 1.5 Hz not even that small amount of noise attenuation was observed. In fact, below 1.5 Hz the greatest attenuation at 60 meters was only about 1.5 db.

It has been verified that a system with about 4 km minimum spacing, such as the Øyer subarray, will result in $\sqrt{N}$ noise rejection in the normal signal band above 0.6 Hz. This was done by making use of frequency wavenumber analysis of the noise as well as by actually forming beams from the Øyer site. This work as well as further frequency wavenumber analysis of Faldalen and Ringsaker data has indicated that surface modes with horizontal phase velocities in the 3 to 4 km/sec range tend to make up the dominant component of organized short-period noise in Norway.

Extreme amplitude variations over the Øyer subarray (approximately 20 km aperture) are approximately a factor of 2 which is to be compared to a factor of 3 for 7-km subarrays in Montana.

Figure 12 shows the typical range of power spectral densities observed in Norway. The curves are uncorrected for instrument response. The general Norway noise level has been verified using more than 20 spectra from the Faldalen noise survey site and a smaller number from the Øyer site. Although the Norway noise level is higher at 1 Hz than it is in Montana, there is a more rapid drop with increasing frequency. Short-period P-magnitudes at Øyer have

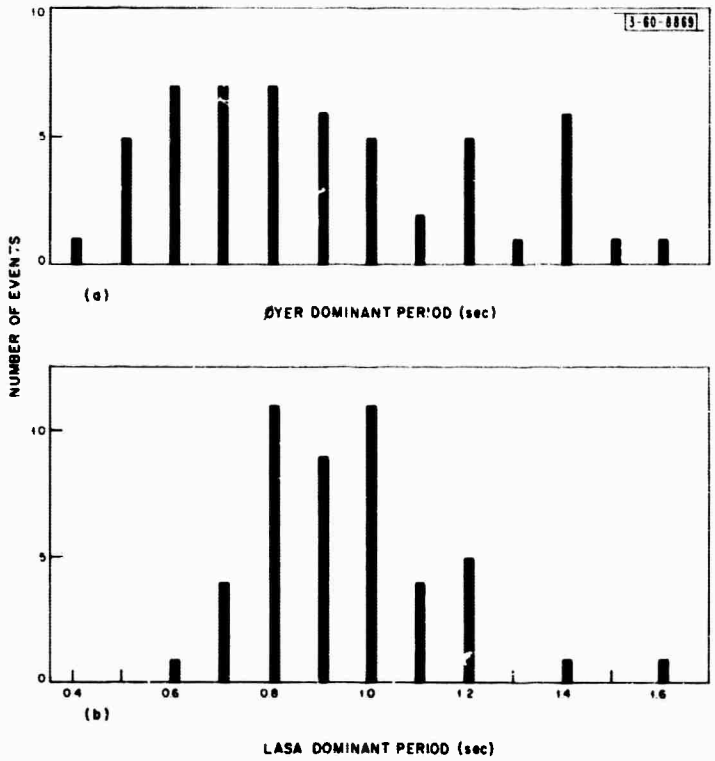

Fig. 13. Spectral differences in P-phase at Norway and Montana in the form of a histogram of dominant periods.

been compared with USCGS magnitudes for 25 events and it was found that the average difference $M_{\text{Dyer}} - M_{\text{CGS}}$ is +0.18 and −0.09 for events from the east (20° – 90°) and west (250° – 310°) respectively, and +0.07 averaged overall azimuths.

One of the most notable differences between signals seen at LASA and NORSAR seems to be the wider spread in the frequency content of the NORSAR signals. Figures 13(a) and (b) show histograms of the dominant periods of a set of events seen at NORSAR and LASA, respectively. The dominant periods at LASA cluster closely around 0.9-second periods while the dominant periods at NORSAR spread from 0.5 to 1.5 seconds.

As another demonstration of the wider variation of spectral characteristics in signals seen at NORSAR compared to those at LASA, Fig. 14(a) and (b) show the spectra of an event in Japan as seen at LASA and NORSAR. For this event, the NORSAR signal has significantly wider bandwidth than the LASA signal. In contrast, Figs. 15(a) and (b) show the spectra of an event in the mid-Atlantic ridge, also approximately equidistant from the two sites, for which the spectra are very similar. It appears that the NORSAR essentially provides a wider band receiver than LASA so that signal characteristics seen at NORSAR may be more influenced by the actual source function than at LASA.

A number of power spectral densities have been estimated using long-period data. The purpose was to obtain information concerning the LP noise level and the relative amounts of noise on vertical and horizontal instruments.

Figures 16(a) and (b) show some of the spectra obtained from three of a total of five observation periods. These spectra are not corrected for instrument response and are relative to 1 $(m\mu)^2$/Hz at 0.04 Hz. The instruments are of the same type as those used in Montana. Other measurements were made for 14 January and 2 February. Figure 16(a) shows spectra for all three components on 28 January which was the observation time which gave the highest noise level. Assuming a signal band from 40- to 20-second periods we note that the peak in-band noise is up to 55 db above the reference level on the vertical instrument and about 50 db on the horizontal instruments. Out of band, the peaks for the 16- and 8-second microseisms are up to almost 60 db on verticals, slightly less on horizontal instruments. Figure 16(b) shows power spectral densities for 28 January as well as for periods about one day earlier and later. The in-band power is reduced from a few to 10 db on those days. The power at 8 and 16 seconds is reduced even more. During this entire 3-day period there was a developed low pressure area just off the northwest coast of Norway, which is thought to be the source of the disturbance. Our observations of spectra on 14 January and 2 February gave noise peaks only up to about 40 db above the reference. A number of observations of LP noise in Montana indicate that the typical in-band vertical noise is about 40 db and that it can be several db higher at the 8 and 16 second peaks.[11] The horizontal noise in Montana is often up to 10 db more intense than the vertical noise.

It appears from the above that the vertical long-period noise component in Norway can be as quiet as typical Montana conditions. However, microseismic storms may be more intense in Norway resulting in vertical noise levels 10 to 20 db higher than those typical in Montana.

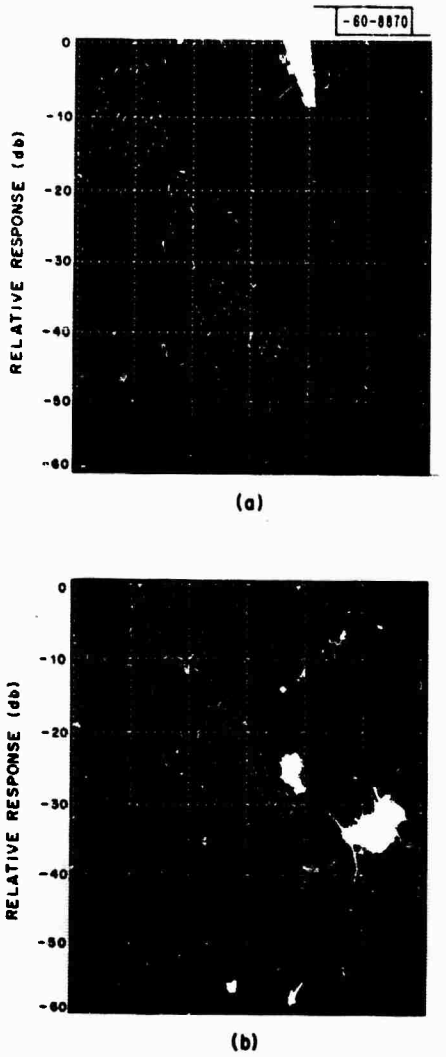

Fig. 14. Comparative spectra of same event at LASA and NORSAR: earthquake off East Coast of Honshu, 11 January 1968, 1612 Z, m_b(LASA) = 4.8. (a) LASA beam, (b) NORSAR Øyer subarray beam.

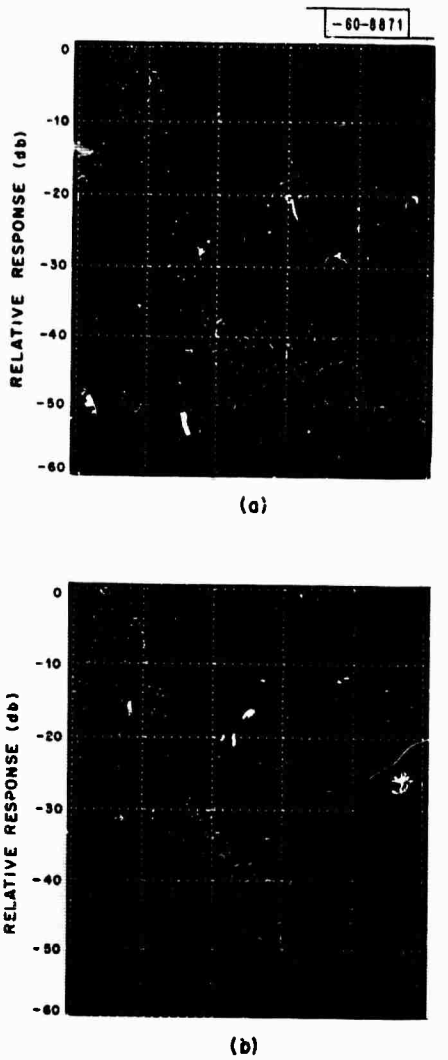

Fig. 15. Comparative spectra of same event at LASA and NORSAR: earthquake on Mid-Atlantic Ridge, 8 January 1968, 2022 Z, m_b(LASA) = 5.3. (a) LASA beam, (b) NORSAR Øyer subarray beam.

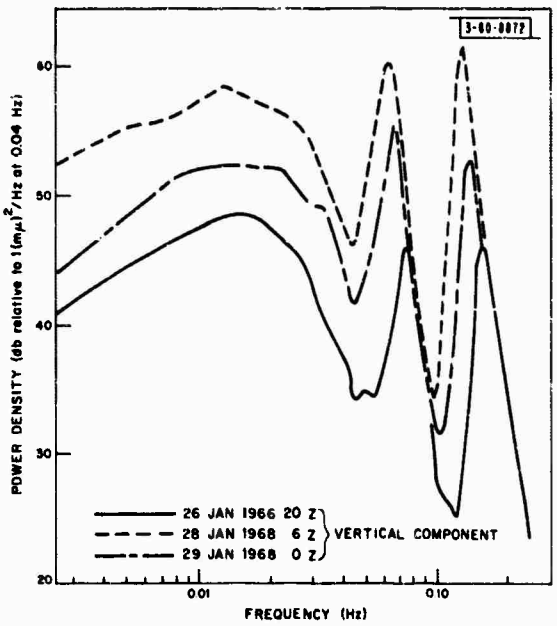

(a) Vertical component before, during and after micraseismic noise peak.

(b) Comparison of vertical and horizontal output at micraseismic storm peak.

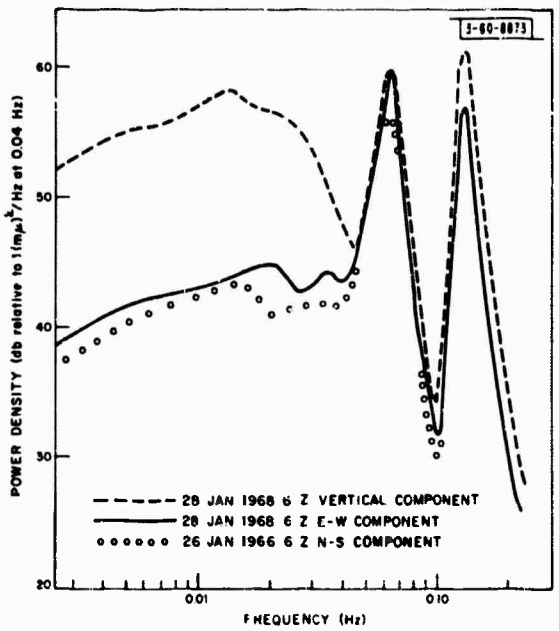

Fig. 16. Norway (Faldalen) LP noise spectra.

Of course, very intense storms can similarly raise noise levels in Montana but the intensity and duration is likely to be greater in Norway. Apparently the horizontal instruments in Norway have somewhat less noise than the verticals. This is particularly true at periods greater than 25 or 30 seconds and when the vertical component noise level is high. The in-band horizontal noise level in Norway is typically a few db less than that in Montana and should never be any worse than the typical Montana level even during intense microseismic storms in Norway.

From a study of surface waves on nine events seen at both NORSAR and LASA, it was found that on the average, M_s values at the two stations are equal.

Attempts to determine the direction and velocity of LP noise in Norway by frequency-wavenumber methods have been without success thus far, due to limited data coverage, small number of sites (three), and large separations (100 km).

H. W. Briscoe
R. T. Lacoss

E. LASA STATION CORRECTION STUDIES

We have not reported on our work with station corrections for several years, although they are basic to the operation of the array and a number of changes have been made in the way they have been measured and used. A description of the work performed in this reporting period will be preceded here by a summary of previous work not mentioned in preceding Semiannual Reports.

When the arrival times of P at each LASA subarray are measured, for a well-recorded event, and compared with the times predicted by standard tables and published source parameters, two kinds of error are observed. First, the arrival time at any given subarray, such as the "reference subarray" A$\emptyset$, differs from the predicted time, and second, the measured moveouts, relative to this reference, differ from the corresponding computed moveouts. The first error contains source parameter errors, propagation anomalies in the vicinity of the source (source correction), departure of actual travel time from world-wide average tables, record reading error, and the absolute station correction, relative to the standard tables used, of the reference subarray. The absolute station correction is presumably due to local propagation anomalies in the vicinity of the reference site, although the separation of "local" effects from "regional travel time variations" is necessarily imprecise. The second error, for any given subarray other than A$\emptyset$, is attributed to the "relative station correction," although all the sources of error enumerated above are present to some degree. One expects that source parameter errors and source corrections are comparatively less important in the relative station correction, and that only departures of travel time derivatives from standard tables will be relevant over the LASA aperture. However, the local propagation anomalies under the subarray in question and under the reference site will both contribute.

Earthquake arrival time data, yielding information on both kinds of station correction, is valuable both for providing insight into the velocity structure under the array and for the operational determination of epicenters by either triangulation or beamsplitting. In this Section we describe our work with this arrival time data, the aim of which is to reduce it to a form more useful for both purposes.

Our earliest work with station corrections was based upon measurements of P arrival times, taken from film recordings at the Laboratory, and reduced to relative station correction data by

the use of USCGS reports on source parameters. The moveout anomaly data was displayed, for each subarray, as a function of event bearing only (since the data depend most strongly on bearing) and fit by least squares to a five-term Fourier series in the bearing angle. Values from the resulting curves were then used for epicenter determination by triangulation. It was evident at once that the results had three shortcomings: (1) the data base of about 150 events was inadequate, (2) it would be necessary to know the station corrections as functions of both distance and bearing, and (3) the extremely non-uniform geographical character of natural seismicity meant that any simple curve- or surface-fitting technique would lead to results dominated by the data from a small fraction of the teleseismic epicentral area.

In order to alleviate the first two shortcomings, we undertook to obtain data on a large population of clearly recorded events and to compute average corrections for each site as functions of distance and bearing. This effort was carried out under subcontract by the Seismic Data Laboratory (Teledyne)[8] and resulted in time and amplituoe anomaly readings for over 600 well-recorded events (of average magnitude 5.1). In order to use the resulting corrections in any location programs, it was necessary either to fit the data with some readily-computable function of two variables, or store the numbers on some fixed grid of points in the distance-bearing plane and use a table lookup procedure when corrections are needed. For the automatic event location program in use at the LASA Data Center, it was decided to use the second approach, although PDP-7 memory limitations restricted us to rather coarse cells. We used 5° in distance and 30° in bearing to define 216 distance-bearing cells, and averaged the raw anomaly measurements over each cell that contained data. At grid points corresponding to cells containing no data, the station corrections were put equal to zero.

The results were fairly satisfactory for triangulation on events which fell in occupied cells, but errors as large as 10° or more could occur for events in unoccupied distance-bearing cells. It was also found that this form of the station corrections was inadequate when patterns of closely-packed beams were formed and their outputs used for epicenter determination, as described in Sec. II-A. On contour plots of beam output energy vs latitude and longitude, abrupt changes at cell boundaries can be seen, especially in the transition from occupied to unoccupied cells.

Our next step (at the beginning of the present reporting period) was to return to the raw station anomaly data (in the form of a tape) and generate histogram displays of the station anomaly for each site. Bounds were then chosen for extreme-value data from each site by studying these histograms, and the data arbitrarily truncated within each pair of bounds. Next, a two-dimensional sliding window, 5° by 5° in the distance-bearing plane was passed over the data to obtain average values on a grid of 1296 distance-bearing pairs. Grid points corresponding to cells containing no data are flagged and station correction numbers for these cells are made up in the following way. First, a value is assigned to each empty cell equal to the average correction for the nearest occupied cell, using great-circle distance on the earth's surface. Next, this complete grid of values is passed repeatedly through a two-dimensional smoothing program which is not allowed to change values corresponding to occupied cells (i.e., real data). The smoothing algorithm is Laplacian; a "new value" is computed for each grid point as the average of the old value and that of its four nearest values, and the smoothed value actually used is a weighted

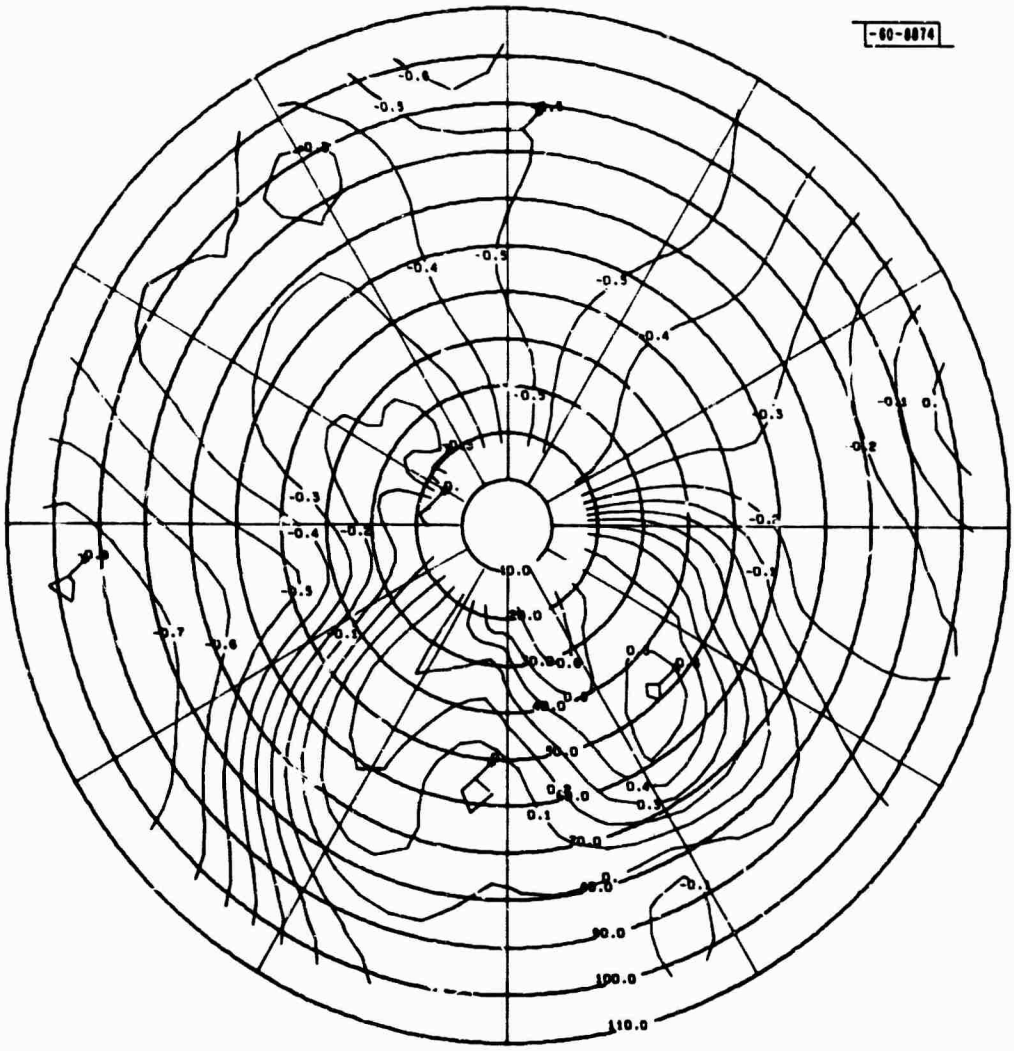

Fig. 17. Smoothed and contoured time station correction of LASA suborray F4 with respect to AØ as a function of epicentrol azimuth and distance.

average of the old and "new" numbers. After many iterations, the result approaches the solution of the finite-mesh Laplace equation with the original real data as boundary values. A moderate amount of smoothing is performed at the end, holding no points fixed. The result is a smooth function of distance and bearing, with values at each grid point and still very close to the original data where such existed. A contour diagram of the F4 correction, using distance and bearing as polar coordinates, is shown in Fig. 17.

The new corrections have so far been used operationally only in beamforming programs, where considerably smoother patterns are now found. However, these interpolated smoothed corrections are also useful in earth structure studies, because they represent the data in a way which is not strongly biased by natural seismicity. One such application is the display of moveout diagrams. These are produced by choosing an epicenter and computing station corrections from the grid values for each site as well as the relative distance of each site to the epicenter. When the corrections are plotted vs projected epicentral distance, the result is a "typical moveout" plot, which is representative of the moveouts obtained for events near that epicenter, with the theoretical moveouts removed. The example shown in Fig. 18, for an epicenter at 72.5°, bearing 145°, clearly suggests a set of dipping layers for the LASA substructure. Attempts to explain the station correction results are being made, based on models of the structure obtained from such moveout plots.

We are now re-referencing station correction data on the 1968 Herrin-Taggart travel times and applying the programs described above to the absolute station correction data at AØ.

E. J. Kelly

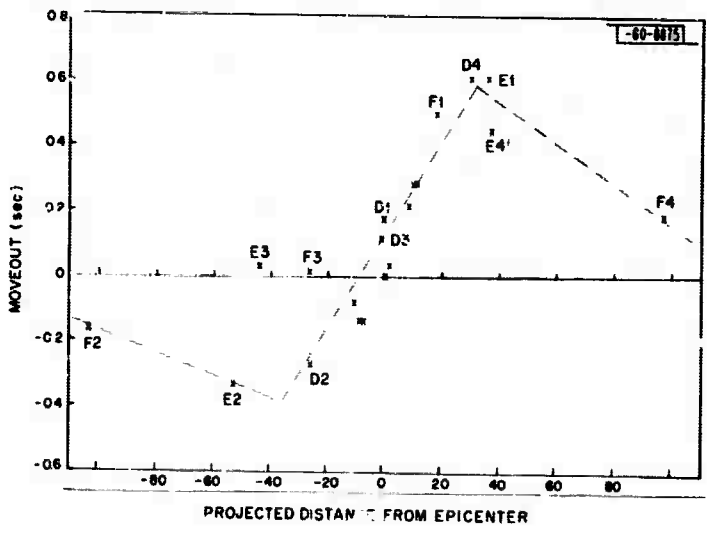

Fig. 18. "Moveout diagram" for bearing 145°, distance 72.5°.

BLANK PAGE

III. GEOPHYSICAL DATA HANDLING TECHNIQUES

A. DATA ANALYSIS CONSOLE

The Data Analysis Console described in the previous Semiannual Technical Summary Report (31 December 1967) has had two programs added to it which are described below. These additions complete the console software design for our present hardware configuration. A complete description of this current system is given in a recent report.[14]

Additional hardware (expanded core memory, 3-million-word drum, automatic priority interrupts and block transfer scope) has been ordered to greatly increase the capability of the basic PDP-7 computer. A new software package will be designed using the new hardware which will create a new data analysis console that will be similar to the one in current use, but will be faster and allow more powerful and versatile processing.

The two new features of the present console are as follows.

1. Event Detecting [J]

This program scans the data tape and types out the time of all teleseisms encountered. The event detection algorithms have been described previously.[15]

2. Matched Filtering [M]

This program cross correlates the reference trace with a matched filter that is specially designed to enhance the SNR of long-period dispersed surface waves.[1] The matched filter is a sinusoid with a linear frequency modulation (chirp). The matched filter has three parameters that can be input to the program via the teletypewriter: the period at the start of the chirp, the period at the end of the chirp, and the length of the chirp. The maximum allowable length of the chirp matched filter impulse response is 800 samples which corresponds to 160 to 1920 seconds depending on the sampling chosen in the Initialize program. Enough of the input reference will be convolved with this chirp to give 512 samples of filtered output, which will appear in the reference buffer.

P. L. Fleck

REFERENCES

1. J. Capon, R. J. Greenfield and R. T. Lacoss, "Long-Period Signal Processing Results for the Large Aperture Seismic Array," Technical Note 1967-50, Lincoln Laboratory, M.I.T. (15 November 1967), DDC 663429.

2. E. J. Kelly, "A Study of Two Short-Period Discriminants," Technical Note 1968-8, Lincoln Laboratory, M.I.T. (12 February 1968), DDC 666701.

3. Semiannual Technical Summary Report to the Advanced Research Projects Agency on Seismic Discrimination, Lincoln Laboratory, M.I.T. (31 December 1967), Sec. V-A, DDC 664872.

4. Semiannual Technical Summary Report to the Advanced Research Projects Agency on Seismic Discrimination, Lincoln Laboratory, M.I.T. (30 June 1967), Sec. II-D, DDC 657327.

5. Semiannual Technical Summary Report to the Advanced Research Projects Agency on Seismic Discrimination, Lincoln Laboratory, M.I.T. (30 June 1964), Sec. III, DDC 443444.

6. Ibid., Sec. II.

7. J. W. Birtill and F. E. Whiteway, "The Application of Phased Arrays to the Analysis of Seismic Body Waves," Phil. Trans. Roy. Soc. A., 258 (1091), 421 (25 November 1965).

8. D. E. Frankowski, private communication.

9. J. G. McDermott, R. J. Labhart and V. O. Marshall, "Preliminary Bulletin, Kurile Island Experiment -- Ocean Bottom Seismographic Experiments," Texas Instruments, Inc. (1 May 1967).

10. R. M. Sheppard, E. J. Kelly and H. W. Briscoe, "Some Observations of Weak Japanese Earthquakes at the Montana LASA," Technical Note 1968-3, Lincoln Laboratory, M.I.T. (8 January 1968), DDC 665122.

11. J. Capon, "Investigation of Long-Period Noise at LASA," Technical Note 1968-15, Lincoln Laboratory, M.I.T. (3 June 1968).

12. R. A. Haubrich and G. S. MacKenzie, "Earth Noise, 5 to 500 Millicycles per Second," J. Geophys. Res. 70 (15 March 1965).

13. Semiannual Technical Summary Report to the Advanced Research Projects Agency on Seismic Discrimination, Lincoln Laboratory, M.I.T. (31 December 1967), Sec. IV-B, DDC 664872.

14. P. L. Fleck, "A Seismic Data Analysis Console," Technical Note 1968-14, Lincoln Laboratory, M.I.T. (13 June 1968).

15. Semiannual Technical Summary Report to the Advanced Research Projects Agency on Seismic Discrimination, Lincoln Laboratory, M.I.T. (31 December 1965), DDC 630559, Sec. III.

DOCUMENT CONTROL DATA – R&D

(Security classification of title, body of abstract and indexing annotation must be entered when the overall report is classified)

1. ORIGINATING ACTIVITY (Corporate author)	2a. REPORT SECURITY CLASSIFICATION
Lincoln Laboratory, M.I.T.	Unclassified
	2b. GROUP: None

3. REPORT TITLE

Semiannual Technical Summary Report to the Advanced Research Projects Agency on Seismic Discrimination

4. DESCRIPTIVE NOTES (Type of report and inclusive dates)

Semiannual Technical Summary Report – 1 January to 30 June 1968

5. AUTHOR(S) (Last name, first name, initial)

Green, Paul E.

6. REPORT DATE	7a. TOTAL NO. OF PAGES	7b. NO. OF REFS
30 June 1968	40	15

8a. CONTRACT OR GRANT NO.	9a. ORIGINATOR'S REPORT NUMBER(S)
AF 19(628)-5167	Semiannual Technical Summary (30 June 1968)
b. PROJECT NO. ARPA Order 512	
c.	9b. OTHER REPORT NO(S) (Any other numbers that may be assigned this report): ESD-TR-68-199
d.	

10. AVAILABILITY/LIMITATION NOTICES

This document has been approved for public release and sale; its distribution is unlimited.

11. SUPPLEMENTARY NOTES	12. SPONSORING MILITARY ACTIVITY
None	Advanced Research Projects Agency, Department of Defense

13. ABSTRACT

Seismic source identification work during this reporting period has involved the development of several new analysis techniques for almost completely automatic production measurement on seismograms, and for less routine, more detailed studies. Studies of array signal detectability and signal and noise spatial character continue using data from both Montana (LASA) and Norway (NORSAR).

14. KEY WORDS

seismic array seismometers seismology